

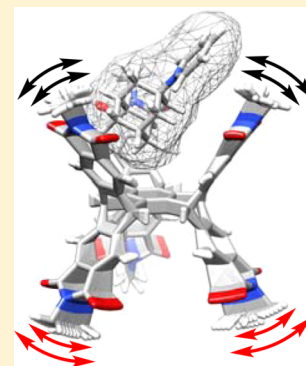
Dual-Cavity Basket Promotes Encapsulation in Water in an Allosteric Fashion

Shigui Chen, Makoto Yamasaki, Shane Polen, Judith Gallucci, Christopher M. Hadad, and Jovica D. Badjić*

Department of Chemistry and Biochemistry, The Ohio State University, 100 West 18th Avenue, Columbus, Ohio 43210, United States

S Supporting Information

ABSTRACT: We prepared dual-cavity basket **1** to carry six (S)-alanine residues at the entrance of its two juxtaposed cavities (289 Å³). With the assistance of ¹H NMR spectroscopy and calorimetry, we found that **1** could trap a single molecule of **4** ($K_1 = 1.45 \pm 0.40 \times 10^4 \text{ M}^{-1}$, ITC), akin in size (241 Å³) and polar characteristics to nerve agent VX (289 Å³). The results of density functional theory calculations (DFT, M06-2X/6-31G*) and experiments (¹H NMR spectroscopy) suggest that the negative homotropic allostery arises from the guest forming C–H⋯π contacts with all three of the aromatic walls of the occupied basket's cavity. In response, the other cavity increases its size and turns rigid to prevent the formation of the ternary complex. A smaller guest **6** (180 Å³), akin in size and polar characteristics to soman (186 Å³), was also found to bind to dual-cavity **1**, although giving both binary [1C6] and ternary [1C6₂] complexes ($K_1 = 7910 \text{ M}^{-1}$ and $K_2 = 2374 \text{ M}^{-1}$, ¹H NMR spectroscopy). In this case, the computational and experimental (¹H NMR spectroscopy) results suggest that only two aromatic walls of the occupied basket's cavity form C–H⋯π contacts with the guest to render the singly occupied host flexible enough to undergo additional structural changes necessary for receiving another guest molecule. The structural adaptivity of dual-cavity baskets of type **1** is unique and important for designing multivalent hosts capable of effectively sequestering targeted guests in an allosteric manner to give stable supramolecular polymers.



INTRODUCTION

Developing prophylactic measures¹ for the effective removal of organophosphorus (OP) nerve agents of G and V type as well as detection of their minute quantities is important for preventing the act of terrorism and chemical warfare.² Currently, the unambiguous detection of toxic OP substances relies on nonportable analytical instrumentation,³ while developing effective measures for their rapid detection and degradation is still a focus of many research efforts.⁴ Indeed, there are elegant examples of synthetic and biological molecules capable of detecting⁵ and degrading nerve agents.⁶ Chemosensors and catalysts often lack chemo/stereoselectivity⁷ for exclusively “picking” desired OPs among other compounds. The sensing problem could, perhaps, be addressed with the application of pattern recognition methods;⁸ however, for catalysis, one could envision a great utility of molecular encapsulation.⁹ Accordingly, we posit¹⁰ that understanding the fundamentals of OP recognition is important for advancing the field. We therefore used molecular baskets equipped with amino acids or amphiphilic groups at the rim for encapsulating OPs.^{10,11} The binding of OP guests is, for such monovalent hosts, described with hyperbolic binding isotherms whereby the complexation event occurs over a broad range of guest concentrations.¹² In the case of multivalent baskets,¹³ however, the complexation of monovalent guests ought to occur in stages¹⁴ with the binding isotherm turning sigmoidal if a strong positive cooperativity ensues.¹⁵ The positive allostery¹⁶ shall

therefore permit tuning “on/off” response of the host,¹⁷ i.e., rapid population switch from mainly bound to unbound or active to inactive structures, and could be of interest for developing switchable¹⁸ and selective sensors¹⁹/catalysts²⁰ capable of effectively detecting/degrading OP nerve agents. In line with this, we hereby describe our findings about characterizing the operation of dual-cavity basket **1** (Figure 1A) in water.¹³ This multivalent host²¹ is chiral, with two juxtaposed cavities and six alanine amino acids at the entrance for the solubility in water. Furthermore, the conformational flexibility of the framework of **1** is critical for tuning the size of the cavities ($V \approx 240 \text{ Å}^3$,²² Figure 1B)^{11c} and therefore accommodating guests²³ in an allosteric fashion.¹⁷

RESULTS AND DISCUSSION

Basket **1** was prepared via Pd(OAc)₂ promoted homocoupling of three bicyclic dibromoalkenes **2**, each possessing two (S)-alanine amino acids (Figure 1A, see also Scheme S1).¹³ The cyclotrimerization of a synthetic precursor of **2** (Scheme S1), however, gave dual-cavity host **3**¹³ akin in shape to basket **1**. Interestingly, single crystal of dual-cavity **3** was obtained by a slow evaporation of a solution of this molecule in CH₃OH/CDCl₃ (Figure 1C, see also Figure S10). The unit cell contains pairs of C₁ symmetric **3**, with two baskets perpendicular to each

Received: June 17, 2015

Published: September 8, 2015

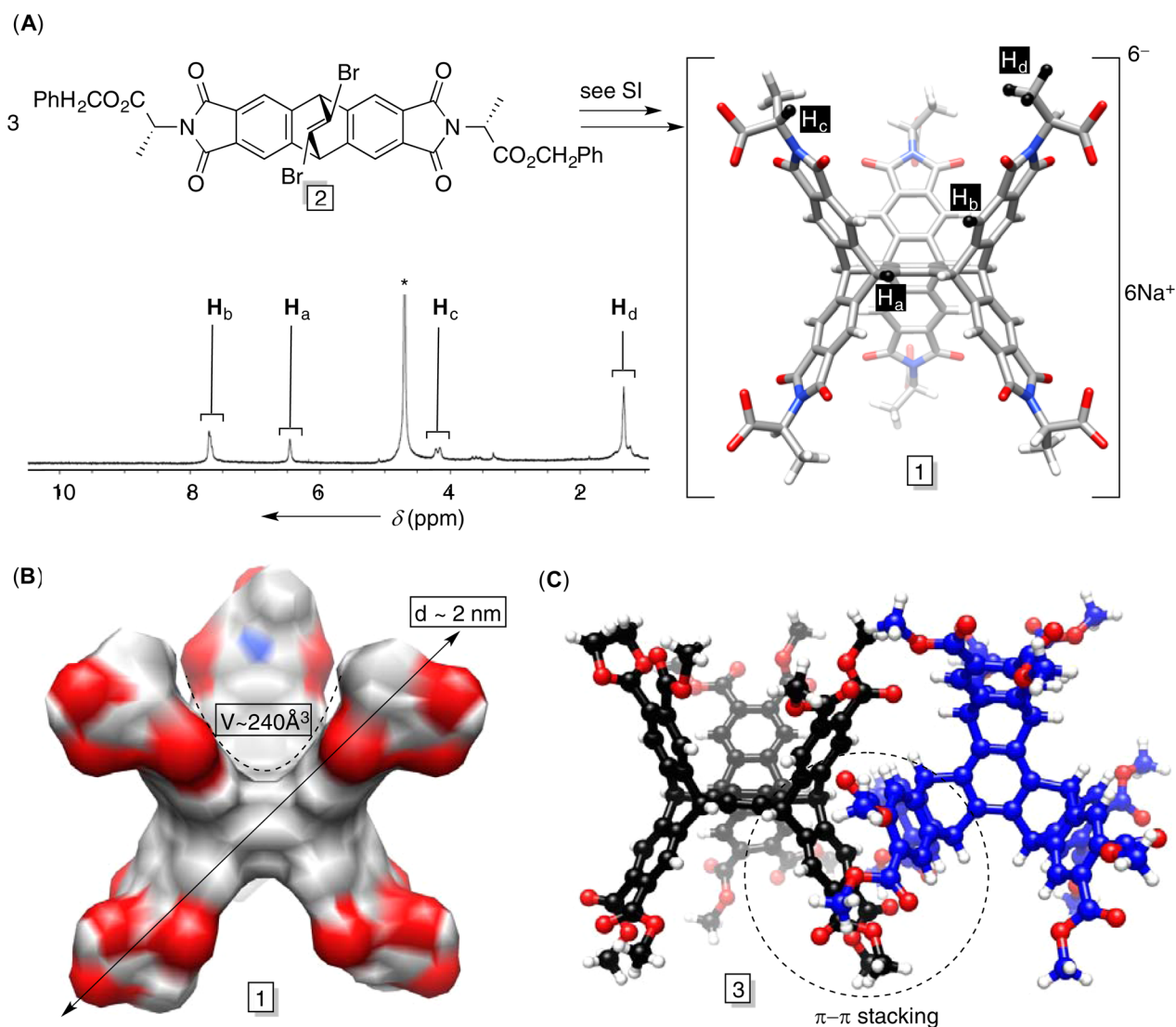


Figure 1. (A) Dual-cavity **1** is obtained from **2** by palladium acetate promoted cyclotrimerization.¹³ ¹³C NMR spectrum (500 MHz, 298.0 K) of **1** (1.0 mM) in D₂O. (B) Van der Waals surface of **1** (MMFFs, Spartan). (C) Solid-state structure of dual-cavity basket **3** (see also Figure S10).

other forming π - π stacking contacts (Figure 1C).²⁴ For one of the baskets, the difference in the averaged length between centroids of its three side aromatics, comprising two juxtaposed cavities, is $\Delta d = 0.5$ Å; for another basket, however, Δd is smaller and equal to 0.1 Å. Evidently, the framework of dual-cavity **3** is flexible enough to, in the solid-state, adjust the size of its concave clefts.²³ Disordered solvent molecules were difficult to locate in the electron density maps, yet some clearly occupy the inner space of **3**. Due to disorder, some carbon and oxygen atoms were isotropically refined contributing to a large *R* factor.

Dual-cavity **1** was soluble in water showing a single set of ¹H NMR resonances (Figure 1A) corresponding to *D*₃ symmetric **1**. A rather broad line width indicates an aggregation^{11a} of this bolaamphiphilic host,²⁵ yet there was no change in the signal for 0.1–5.0 mM solutions of **1** (Figure S3). Importantly, the results of ¹H NMR diffusion ordered spectroscopy (DOSY) measurements²⁶ of **1** in D₂O revealed that the apparent diffusion coefficient stayed practically constant ($D_{app} = 1.8$ – 1.9×10^{-10} m²/s, 298.0 K) across a 0.5–5.0 mM concentration range. The hydrodynamic radii ($R_H = 1.3$ – 1.4 nm) corresponding to such diffusion mobility may suggest the existence of monomeric host or stable aggregates since the

radius of energy-minimized **1** (MMFFs, Spartan, Figure 1B) is estimated to be 1 nm.^{11d}

For studying the encapsulation characteristics of **1**, we first selected adamantane derivative **4**. Importantly, the volume of this guest (241 Å³) as well as its C–H “decorated” hydrophobic moiety (see Figure 2C) resemble the nerve agent VX (289 Å³).¹⁰ An incremental addition of the standard solution of **4** (60.0 mM) to **1** (0.61 mM) in water was monitored with ¹H NMR spectroscopy (600 MHz, Figure 2A; see also Figure S4). A large upfield shift of all proton resonances of **4** suggested the formation of an encapsulation complex, with guest’s protons being magnetically shielded by the host’s aromatics (Figure 2A). The method of continuous variation (Figure 2B) indicated that a 1:1, but not 1:2, complex dominates in solution: the bell-shaped curve peaks at equimolar (ca. 0.5) host–guest ratio.²⁷ In fact, the nonlinear least-squares fitting of ¹H NMR titration data to a 1:1 stoichiometric model gave the association constant $K_1 = 2.2$ – 4.1×10^3 M⁻¹ ($R^2 = 0.99$ with 10% of the standard fitting error; Figure 2A).²⁸ The encapsulation was subsequently monitored with isothermal titration calorimetry (ITC, Figure S5), corroborating the exclusive formation of [**1C4**] and providing thermodynamic data pertaining to the host–guest

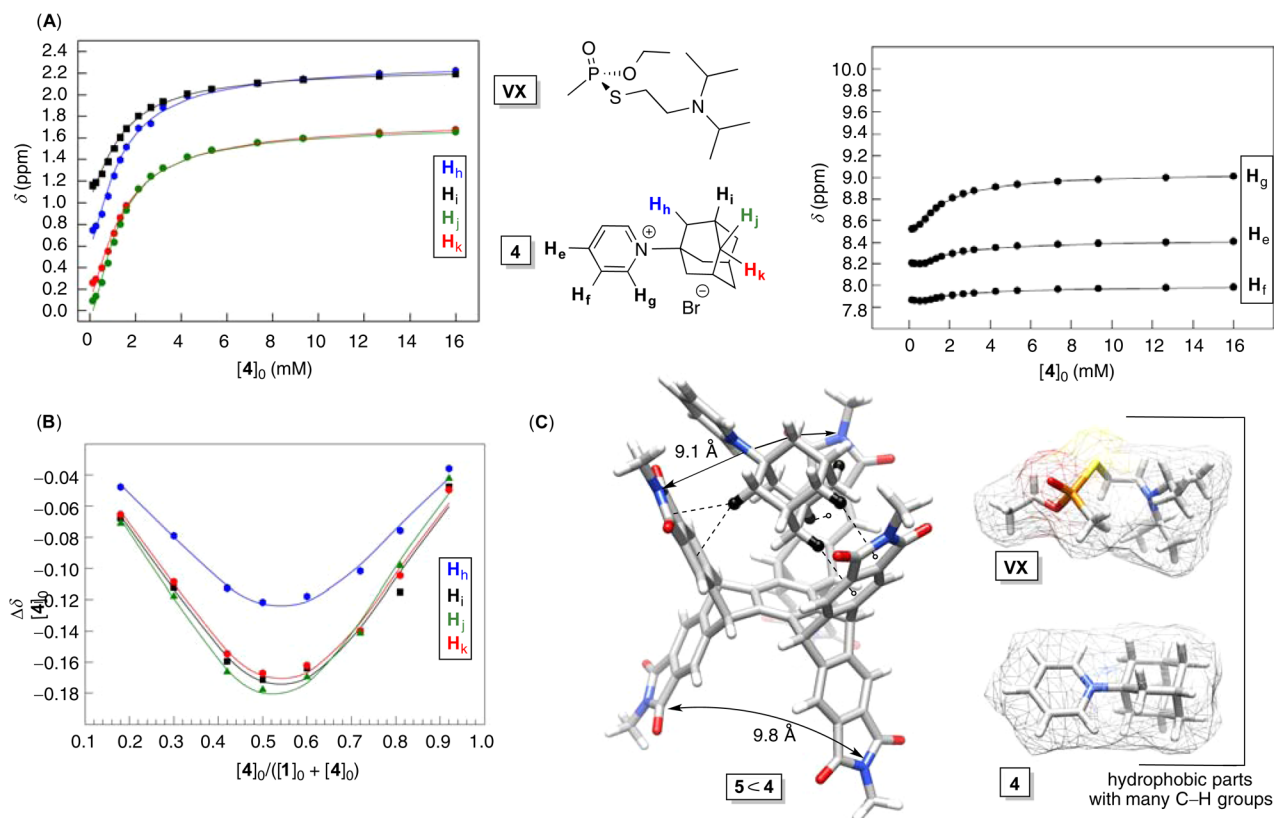


Figure 2. (A) Nonlinear least-squares analysis of H_h – H_k binding isotherms pertaining to the formation of $[1C4]$ (298.0 K) gave the association constant $K_1 = 2.2$ – $4.1 \times 10^3 \text{ M}^{-1}$ ($R^2 = 0.99$ with 10% of the standard fitting error; SigmaPlot). (B) The Job plot corresponding to the formation of $[1C4]$ was obtained using ^1H NMR chemical shifts of signals corresponding to guest **4** ($[1]_0 + [4]_0 = 0.4 \text{ mM}$). (C) A stick representation of energy-minimized $[5C4]$ (DFT, M06-2X/6-31G*) in water showing the guest forming C–H $\cdots\pi$ contacts with all three aromatic walls of the host's one cavity to alter the size of both cavities. Energy-minimized structures of VX (289 \AA^3) and **4** (241 \AA^3), showing their van der Waals surfaces and also depicting a number of C–H groups protruding from the hydrophobic part of each molecule.

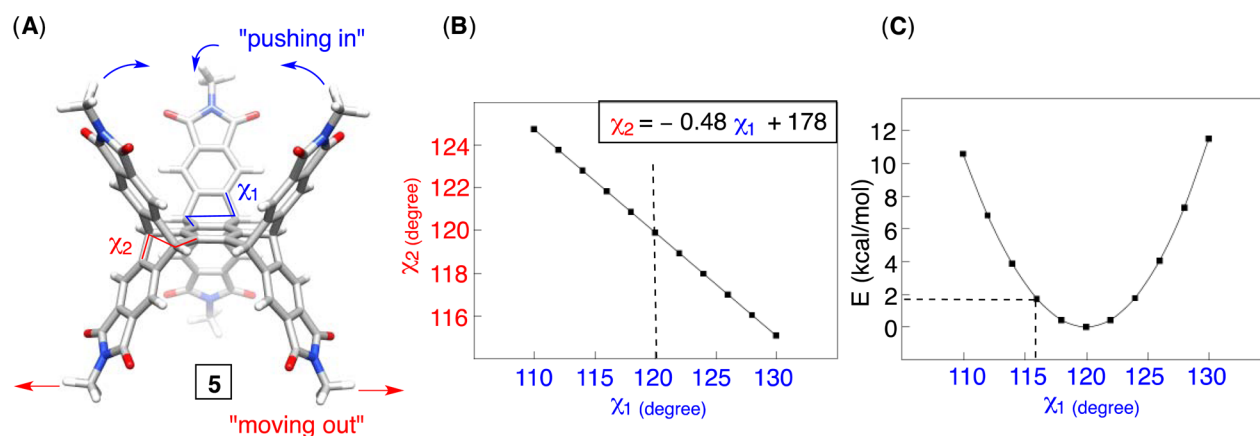


Figure 3. (A) Stick representation of energy-minimized model compound **5** (DFT, B3LYP/6-31G*) showing dihedral angles χ_1 (blue, top) and χ_2 (red, bottom). When one torsion is fixed (χ_1) to a particular value, the energy optimization shows that another dihedral (χ_2) changes correspondingly (B) as well as the total energy of the system (C).

event. The binding ($K_1 = 1.45 \pm 0.40 \times 10^4 \text{ M}^{-1}$, $R^2 = 0.95$; Figure S5) is driven by entropy ($T\Delta S^\circ = 6.6 \pm 0.3 \text{ kcal/mol}$, 298.0 K) while the change in enthalpy is positive ($\Delta H^\circ = 0.96 \pm 0.01 \text{ kcal/mol}$); we reason that an apparent discrepancy between the results of NMR and ITC binding studies is likely due to (a) the fitting of the NMR data to the chemical shift of guest protons in the experiment in which the guest is added to the host²⁸ and (b) rather poor signal-to-noise ratio and a broadening of proton resonances. Apparently, the classical

hydrophobic effect²⁹ and therefore a desolvation of primarily hydrophobic regions of the host/guest pair are driving the formation of the noncovalent complex.^{11b} The degree of perturbation of ^1H NMR signals of **4**, characterizing its entrapment (Figure 2A), is in line with this interpretation. That is to say, the ^1H resonances corresponding to nuclei $H_h/H_i/H_j/H_k$ within the adamantane moiety in **4** are shielded to a greater degree ($\Delta\delta = 1.1$ – 1.6 ppm , Figure 2A) than those of $H_e/H_f/H_i/H_j$ within the pyridinium group ($\Delta\delta = 0.1$ – 0.5 ppm , Figure 2A). It

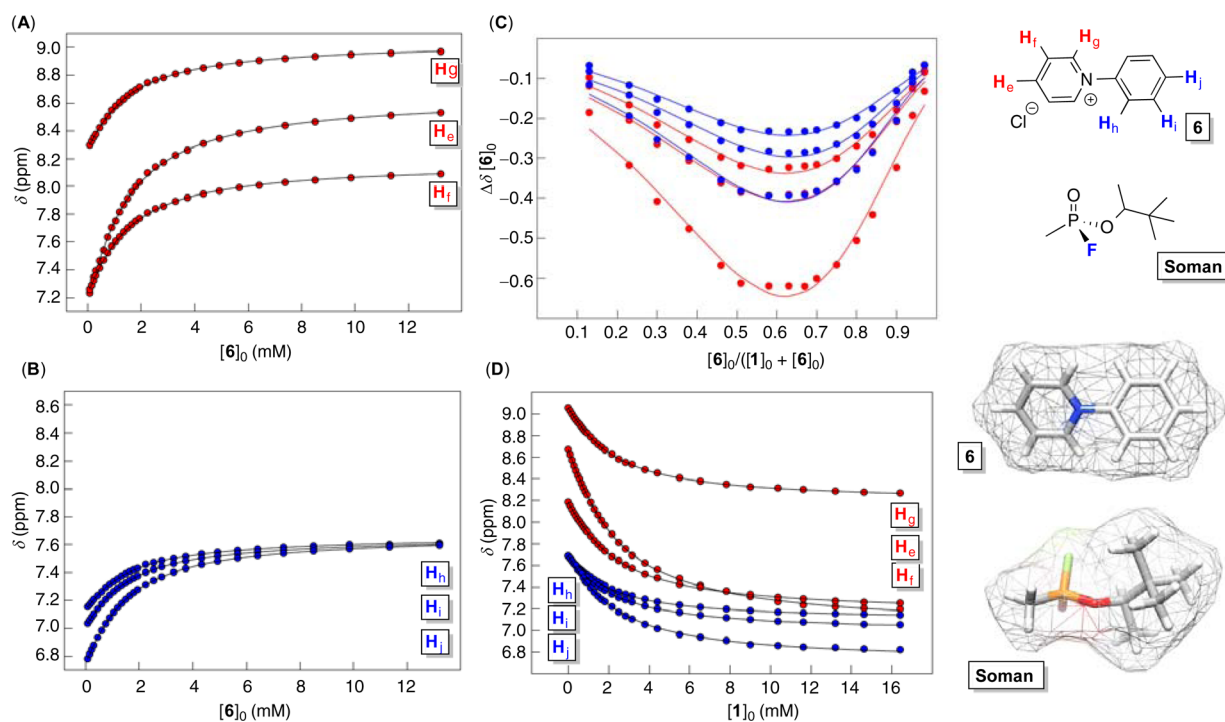


Figure 4. (A, B) ^1H NMR chemical shifts (600 MHz) of resonances corresponding to protons of **6** as its solution (31.3 mM) was incrementally added to dual-cavity **1** (0.5 mM) in D_2O at 298.0 K. (C) The Job plot describing to the formation of ternary $[\text{1C6}_2]$ was obtained using ^1H NMR chemical shifts of signals corresponding to guest **6** ($[\text{1}]_0 + [\text{6}]_0 = 0.4 \text{ mM}$).²⁷ (D) Nonlinear least-squares analysis of binding isotherms pertaining the formation of $[\text{1C6}]/[\text{1C6}_2]$ gave association constants K_1 and K_2 for two subsequent binding events.³² Energy-minimized structures of guest **6** and soman (MMFFs, Spartan), showing their van der Waals surfaces and polar/nonpolar zones.

follows that more hydrophobic adamantane in the guest is residing in the arene-based cavity of the host. Why does negative homotropic allostery³⁰ take place with the predominant formation of $[\text{1C4}]$ and absence of $[\text{1C4}_2]$? To address this question, we first used density functional theory (DFT, B3LYP/6-31G*)³¹ to study the conformational dynamics of the framework of model dual-cavity **5** (Figure 3A). The concave portion of this host is the same as in basket **1**, although it is lacking six negatively charged carboxylate groups to facilitate the computational studies: the carboxylates serve to improve the solubility of dual-cavity **1** and are hypothesized to play a minor role in the recognition occurring in polar water environment. Top and bottom torsions χ_1 and χ_2 (Figure 3A) within **5** depict the size of the juxtaposed cavities and are identical for the energy-minimized host (χ_1 and $\chi_2 = 120^\circ$). When the top torsion χ_1 was, however, constrained to a particular value and the energy minimization conducted, the bottom torsion χ_2 would undergo a correlated change following a linear dependence (Figure 3B). Thus, “squeezing” the top cavity (reducing χ_1) causes an expansion of the bottom one (increasing χ_2) and vice versa (Figure 3B). The total host’s energy E as a function of χ_1 fits a cubic polynomial (Figure 3C), with a relatively small energy fluctuation ($dE/d\chi_1 \rightarrow 0$) about the energy minimum ($\chi_1 = 120^\circ$, Figure 3C). The framework of model **5**, akin to **1**, is flexible²³ with 1.7 kcal/mol needed to “squeeze” the top cavity by $\Delta\chi_1 = 4^\circ$ and thereby bring three imide nitrogen atoms on top to $d_{\text{N/N}} = 9.0 \text{ \AA}$ while concurrently separating those at the bottom to $d_{\text{N/N}} = 10.1 \text{ \AA}$ (Figure 3C)! Then, we used M06-2X/6-31G*³³ calculations to examine the encapsulation of **4** inside the cavity of model basket **5**. The most stable coconformation³⁴ (carcerisomer)³⁵ of $[\text{5C4}]$ comprises an adamantane moiety holding against all three of

the host’s aromatic walls by forming numerous $\text{C-H}\cdots\pi$ contacts ($d(\text{C-H}\cdots\text{Csp}^2) < 3.05 \text{ \AA}$, Figure 2C).³⁶ In this way, the occupied cavity becomes contracted ($d_{\text{N/N}} = 9.1 \text{ \AA}$, Figure 2C) while concurrently the vacant one increases its size ($d_{\text{N/N}} = 9.8 \text{ \AA}$, Figure 2C). Since the adamantane group in **4** is also occupying the cavity of **1**, we presume that the same type of conformational change is taking place with the experimentally examined $[\text{1C4}]$ complex. It follows that the observed negative homotropic allostery, and the absence of $[\text{1C4}_2]$, arises from dual-cavity **1** requiring all three of its aromatic walls, within one cavity (Figure 2C), to interact with the guest. As this cavity is reducing its size, in an induced-fit fashion,³⁷ the other one becomes bigger and incapable of forming sufficient number of $\text{C-H}\cdots\pi$ contacts to stay occupied. In fact, the computed binding energies (M06-2X/6-31G*) for the formation of $[\text{5C4}]$ ($\Delta E = -15.44 \text{ kcal/mol}$, Table S3) and $[\text{5C4}_2]$ ($\Delta E = -11.65 \text{ kcal/mol}$, Table S3), in implicit water solvent, suggest a greater stability of the binary complex: to retain numerous $\text{C-H}\cdots\pi$ contacts, one of the cavities is in $[\text{5C4}_2]$ still more ($d_{\text{N/N}} = 9.1 \text{ \AA}$, Figure S11) contracted than the other ($d_{\text{N/N}} = 9.4 \text{ \AA}$, Figure S11). The effective formation of ternary $[\text{5C4}_2]$ requires for the “cups” to be similar in size, which clearly comes at the energetic cost of straining the basket’s framework. In general, when the dual-cavity basket is forming a “tight” 1:1 complex with the involvement of all three aromatic walls from one of its “cups”, binding of a second identical guest is not to be expected. Finally, preorganized complex $[\text{1C4}]$ ³⁸ could elicit a selective encapsulation of more sizable and complementary molecules of interest¹¹ to give a stable ternary complex³⁹ or even more elaborate assemblies.¹⁷

To additionally examine the allosteric operation of **1**, we studied the encapsulation of phenylpyridinium guest **6** (180 \AA^3 ,

Figure 4) akin in size and polar characteristics to nerve agent soman (186 \AA^3);¹⁰ note that these two molecules possess polar and nonpolar zones of a comparable size (Figure 4). The hypothesis was that less sizable compound **6** would form fewer contacts²⁴ with **1**, which could possibly give rise to ternary $[\text{1C6}_2]$ complex. An incremental addition of the standard solution of **6** (31.3 mM) to **1** (0.5 mM) in D_2O was monitored with ^1H NMR spectroscopy (Figure 4A,B, see also Figure S6). An upfield shift of all of the guest's resonances is in line with an inclusion of **6** in the cavity of **1**. In fact, the Job plot is indicative of the formation of ternary $[\text{1C6}_2]$ complex with the parabola peaking at approximate 1:2 host/guest ratio (0.67, Figure 4C). A greater upfield perturbation (on average) of resonances $\text{H}_g/\text{H}_e/\text{H}_f$ ($\Delta\delta = 0.7\text{--}1.3$ ppm, Figure 4A) than those of $\text{H}_h/\text{H}_i/\text{H}_j$ ($\Delta\delta = 0.5\text{--}0.8$ ppm, Figure 4B) suggests the predominant disposition of pyridinium moiety inside the aromatic cavity of **1**. In fact, the complexation-induced shift of H_e resonance is by far the greatest (1.30 ppm), with this proton of the guest embedded in the cavity of **1** more deeply than the others. A small change in the chemical shift of ^1H NMR resonances of the host (Figure S6), however, prevented us from quantifying two consecutive binding events K_1 and K_2 . In line with it, the calorimetry measurements (ITC) were giving scattered data points due to a small heat of complexation (Figure S7), while the electronic spectrum of **1** was practically unperturbed upon the complex formation (Figure S8). Accordingly, we decided to complete a "reverse" ^1H NMR titration with an incremental addition of the standard solution of host **1** (4.0 mM) to guest **6** (0.25 mM) in D_2O (Figure 4D, see also Figure S9). Nonlinear least-squares analysis of binding isotherms (Figure 4D),³² to 2:1 stoichiometric model, was satisfactory (cov fit = 0.0003)³² with $K_1 = 7910 \text{ M}^{-1}$ corresponding to the stability of $[\text{1C6}]$ and $K_2 = 2374 \text{ M}^{-1}$ describing the formation of $[\text{1C6}_2]$; the fitting of the data was initiated with the ratio of variables K_1/K_2 , originally set to 4:1. Since the ratio of two consecutive association constants is $K_1/K_2 = 3.3$, and smaller than 4, the binding is positively cooperative albeit close to the statistical one.⁴⁰ The origin of the effect is, at present, difficult to computationally/experimentally elucidate yet our preliminary studies of dual-cavity **1** complexing a dimeric form of compound **6** indicate the formation of supramolecular polymers⁴¹ to vindicate the binding analysis. The computational study of model complex $[\text{5C6}]$ (M06-2X/6-31G*, Figure 5)³³ shows guest **6** positioning its pyridinium group against one of the basket's aromatic walls at centroid-to-centroid distance of 3.7 \AA .²⁴ Furthermore, $\text{C}\text{--}\text{H}\cdots\pi$ interactions^{36b} with the bottom benzene ring and two side aromatic walls hold the guest molecule in its place (Figure 5). If two aromatic walls are in $[\text{1C6}]$ restrained, then one aromatic wall remains "disconnected" (shown as green for model $[\text{5C6}]$, Figure 5). This particular unit of the host is conformationally more flexible, and it ought to be able to adjust in response to another guest to allow for the formation of ternary complex. In brief, singly occupied $[\text{1C6}]$ comprises a more adaptable organic framework capable of accommodating another guest of the same type and giving $[\text{1C6}_2]$!

CONCLUSION

In conclusion, dual-cavity **1** ($V \approx 240 \text{ \AA}^3$) is a modular, adaptable, and chiral host capable of trapping guests, akin in size and polarity to nerve agents ($186\text{--}289 \text{ \AA}^3$), in water via hydrophobic effect. When a guest molecule effectively populates one cavity of **1**, it forms $\text{C}\text{--}\text{H}\cdots\pi$ noncovalent

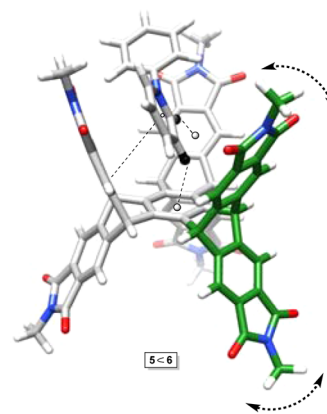


Figure 5. Stick representation of energy-minimized $[\text{5C6}]$ (DFT, M06-2X/6-31G*) showing the guest forming $\text{C}\text{--}\text{H}\cdots\pi$ contacts with the bottom benzene ring and back aromatic wall of the host in addition to $\pi\text{--}\pi$ stacking contacts with the aromatic group on the left. One aromatic wall in the top cavity (green) is practically not interacting with the guest.

contacts with all three of its aromatic walls. As a result, the other cavity changes its size and turns rigid to prevent additional encapsulation leading to negative homotropic allosterism. If the targeted guest is smaller, however, it interacts with only one or two aromatic walls of the basket's cavity to render the singly occupied host flexible enough to undergo additional structural changes necessary for receiving another guest molecule of the same type. The structural adaptivity of dual-cavity baskets of type **1** is unique⁴² and important for designing multivalent hosts capable of effectively sequestering targeted nerve agents in an allosteric fashion and via hydrophobic effect, to eventually give stable supramolecular polymers⁴¹ in water. The work in our laboratories continues toward achieving such goals.

ASSOCIATED CONTENT

Supporting Information

The Supporting Information is available free of charge on the ACS Publications website at DOI: 10.1021/jacs.5b06041.

Crystallographic data (CIF)

Additional details of the experimental and computational protocols (PDF)

AUTHOR INFORMATION

Corresponding Author

*badjic@chemistry.ohio-state.edu

Funding

The experimental portion of this work was financially supported with funds obtained from the U.S. National Science Foundation (CHE-1305179). The computational part was financially supported with funds obtained from the Department of Defense, Defense Threat Reduction Agency (HDTRA1-11-1-0042). Computational support from the Ohio Supercomputer Center is gratefully acknowledged.

Notes

The authors declare no competing financial interest.

REFERENCES

- (1) Rauschel, F. M. *Nature* **2011**, *469*, 310–311.
- (2) Kim, K.; Tsay, O. G.; Atwood, D. A.; Churchill, D. G. *Chem. Rev.* **2011**, *111*, 5345–5403.

- (3) Cordell, R. L.; Willis, K. A.; Wyche, K. P.; Blake, R. S.; Ellis, A. M.; Monks, P. S. *Anal. Chem.* **2007**, *79*, 8359–8366.
- (4) Smith, B. M. *Chem. Soc. Rev.* **2008**, *37*, 470–478.
- (5) (a) Ajami, D.; Rebek, J. *Org. Biomol. Chem.* **2013**, *11*, 3936–3942. (b) Chen, S.; Cashman, J. R. *Adv. Mol. Toxicol.* **2013**, *7*, 207–233.
- (6) Mondloch, J. E.; Katz, M. J.; Isley, W. C., III; Ghosh, P.; Liao, P.; Bury, W.; Wagner, G. W.; Hall, M. G.; De Coste, J. B.; Peterson, G. W.; Snurr, R. Q.; Cramer, C. J.; Hupp, J. T.; Farha, O. K. *Nat. Mater.* **2015**, *14*, 512–516.
- (7) Benschop, H. P.; De Jong, L. P. A. *Acc. Chem. Res.* **1988**, *21*, 368–374.
- (8) Askim, J. R.; Mahmoudi, M.; Suslick, K. S. *Chem. Soc. Rev.* **2013**, *42*, 8649–8682.
- (9) Chulvi, K.; Gavina, P.; Costero, A. M.; Gil, S.; Parra, M.; Gotor, R.; Royo, S.; Martinez-Manez, R.; Sancenon, F.; Vivancos, J.-L. *Chem. Commun.* **2012**, *48*, 10105–10107.
- (10) Ruan, Y.; Taha, H. A.; Yoder, R. J.; Maslak, V.; Hadad, C. M.; Badjic, J. D. *J. Phys. Chem. B* **2013**, *117*, 3240–3249.
- (11) (a) Chen, S.; Ruan, Y.; Brown, J. D.; Gallucci, J.; Maslak, V.; Hadad, C. M.; Badjic, J. D. *J. Am. Chem. Soc.* **2013**, *135*, 14964–14967. (b) Chen, S.; Ruan, Y.; Brown, J. D.; Hadad, C. M.; Badjic, J. D. *J. Am. Chem. Soc.* **2014**, *136*, 17337–17342. (c) Ruan, Y.; Chen, S.; Brown, J. D.; Hadad, C. M.; Badjic, J. D. *Org. Lett.* **2015**, *17*, 852–855. (d) Ruan, Y.; Dalkilic, E.; Peterson, P. W.; Pandit, A.; Dastan, A.; Brown, J. D.; Polen, S. M.; Hadad, C. M.; Badjic, J. D. *Chem. - Eur. J.* **2014**, *20*, 4251–4256.
- (12) Riddle, J. A.; Jiang, X.; Lee, D. *Analyst* **2008**, *133*, 417–422.
- (13) Hermann, K.; Sardini, S.; Ruan, Y.; Yoder, R. J.; Chakraborty, M.; Vyas, S.; Hadad, C. M.; Badjic, J. D. *J. Org. Chem.* **2013**, *78*, 2984–2991.
- (14) Ercolani, G. *J. Am. Chem. Soc.* **2003**, *125*, 16097–16103.
- (15) Hunter, C. A.; Anderson, H. L. *Angew. Chem., Int. Ed.* **2009**, *48*, 7488–7499.
- (16) Perlmutter-Hayman, B. *Acc. Chem. Res.* **1986**, *19*, 90–96.
- (17) Takeuchi, M.; Ikeda, M.; Sugasaki, A.; Shinkai, S. *Acc. Chem. Res.* **2001**, *34*, 865–873.
- (18) Ramsay, W. J.; Nitschke, J. R. *J. Am. Chem. Soc.* **2014**, *136*, 7038–7043.
- (19) (a) Zhu, L.; Anslyn, E. V. *Angew. Chem., Int. Ed.* **2006**, *45*, 1190–1196. (b) Saha, I.; Lee, J. H.; Hwang, H.; Kim, T. S.; Lee, C.-H. *Chem. Commun.* **2015**, *51*, 5679–5682.
- (20) Gianneschi, N. C.; Bertin, P. A.; Nguyen, S. T.; Mirkin, C. A.; Zakharov, L. N.; Rheingold, A. L. *J. Am. Chem. Soc.* **2003**, *125*, 10508–10509.
- (21) Mammen, M.; Choi, S.-K.; Whitesides, G. M. *Angew. Chem., Int. Ed.* **1998**, *37*, 2754–2794.
- (22) Voss, N. R.; Gerstein, M. *Nucleic Acids Res.* **2010**, *38*, W555–W562.
- (23) Venugopalan, P.; Buerger, H.-B.; Frank, N. L.; Baldrige, K. K.; Siegel, J. S. *Tetrahedron Lett.* **1995**, *36*, 2419–2422.
- (24) Meyer, E. A.; Castellano, R. K.; Diederich, F. *Angew. Chem., Int. Ed.* **2003**, *42*, 4120.
- (25) Yu, G.; Jie, K.; Huang, F. *Chem. Rev.* **2015**, *115*, 7240.
- (26) Cohen, Y.; Avram, L.; Frish, L. *Angew. Chem., Int. Ed.* **2005**, *44*, 520–554.
- (27) Hirose, K. *Anal. Methods Supramol. Chem.* **2007**, 17–54.
- (28) *Frontiers in Supramolecular Organic Chemistry and Photochemistry*; Schneider, H. J., Duerr, H., Eds.; VCH: Weinheim, 1991.
- (29) Gibb, B. C. *Chemosensors* **2011**, 3–18.
- (30) (a) Thordarson, P.; Bijsterveld, E. J. A.; Elemans, J. A. A. W.; Kasak, P.; Nolte, R. J. M.; Rowan, A. E. *J. Am. Chem. Soc.* **2003**, *125*, 1186–1187. (b) Nabeshima, T.; Yoshihira, Y.; Saiki, T.; Akine, S.; Horn, E. *J. Am. Chem. Soc.* **2003**, *125*, 28–29.
- (31) Lee, C.; Yang, W.; Parr, R. G. *Phys. Rev. B: Condens. Matter Mater. Phys.* **1988**, *37*, 785–789.
- (32) Thordarson, P. *Chem. Soc. Rev.* **2011**, *40*, 1305–1323.
- (33) Zhao, Y.; Truhlar, D. G. *Theor. Chem. Acc.* **2008**, *120*, 215–241.
- (34) Badjic, J. D.; Balzani, V.; Credi, A.; Lowe, J. N.; Silvi, S.; Stoddart, J. F. *Chem. - Eur. J.* **2004**, *10*, 1926–1935.
- (35) Timmerman, P.; Verboom, W.; van Veggel, F. C. J. M.; van Duynhoven, J. P. M.; Reinhoudt, D. N. *Angew. Chem.* **1994**, *106*, 2437–2440.
- (36) (a) Nishio, M.; Umezawa, Y.; Fantini, J.; Weiss, M. S.; Chakrabarti, P. *Phys. Chem. Chem. Phys.* **2014**, *16*, 12648–12683. (b) Ruan, Y.; Peterson, P. W.; Hadad, C. M.; Badjic, J. D. *Chem. Commun.* **2014**, *50*, 9086–9089.
- (37) (a) Hiraoka, S.; Harano, K.; Nakamura, T.; Shiro, M.; Shionoya, M. *Angew. Chem., Int. Ed.* **2009**, *48*, 7006–7009. (b) Corbett, P. T.; Tong, L. H.; Sanders, J. K. M.; Otto, S. J. *Am. Chem. Soc.* **2005**, *127*, 8902–8903.
- (38) Wittenberg, J. B.; Isaacs, L. *Supramol. Chem. Mol. Nanomater.* **2012**, *1*, 25–43.
- (39) Thordarson, P.; Coumans, R. G. E.; Elemans, J. A. A.; Thomassen, P. J.; Visser, J.; Rowan, A. E.; Nolte, R. J. M. *Angew. Chem., Int. Ed.* **2004**, *43*, 4755–4759.
- (40) Badjic, J. D.; Nelson, A.; Cantrill, S. J.; Turnbull, W. B.; Stoddart, J. F. *Acc. Chem. Res.* **2005**, *38*, 723–732.
- (41) Aida, T.; Meijer, E. W.; Stupp, S. I. *Science* **2012**, *335*, 813–817.
- (42) Kao, M.-T.; Chen, J.-H.; Chu, Y.-Y.; Tseng, K.-P.; Hsu, C.-H.; Wong, K.-T.; Chang, C.-W.; Hsu, C.-P.; Liu, Y.-H. *Org. Lett.* **2011**, *13*, 1714–1717.